DOI: 10.2478/aucts-2024-0011

ACTA UNIVERSITATIS CIBINIENSIS – TECHNICAL SERIES
Vol. 76 2024

OPTIMIZED DIMENSIONING AND ENCODER CONFIGURATION FOR AGV TRACTION SYSTEMS

MAGA Vasile Alexandru
Faculty of Engineering/Department of Machines and Industrial Equipment, "Lucian Blaga" University, Sibiu, Romania, vasilealexandru.maga@ulbsibiu.ro

CRENGANIS Mihai *[1]
Faculty of Engineering/Department of Machines and Industrial Equipment, "Lucian Blaga" University, Sibiu, Romania, mihai.crenganis@ulbsibiu.ro, * corresponding author

Abstract: *This study focuses on the meticulous design and dimensioning of the drive system and encoder setup for an Automated Guided Vehicle (AGV) intended for industrial material handling and transportation. The chosen drive system employs a differential traction mechanism, integrated with two brushless hub motors, which offers a balance of high efficiency, low maintenance, and exceptional durability. These motors are specifically selected to meet stringent requirements related to payload, terrain adaptability, torque, and speed.*

The dimensioning process accounts for factors such as rolling friction, incline resistance, and operational speeds, ensuring optimal motor performance under varying conditions. Calculations for torque, power, and speed requirements are presented in detail, highlighting the precision involved in selecting motor specifications that align with the platform's operational goals.

To enhance navigational accuracy, a dead wheel encoder system is incorporated, addressing the inherent limitations of wheel slippage in odometry measurements. The study elaborates on the encoder selection process, emphasizing the importance of resolution and configuration to meet the desired stopping precision. A comparison between built-in motor encoders and external dead wheel encoders illustrates the improvements achieved in positional accuracy.

The paper concludes with insights into the decision-making process for component selection, supported by comprehensive calculations and design considerations. The resulting AGV drive system not only meets the technical demands of industrial environments but also demonstrates scalability and cost-effectiveness, offering a robust foundation for future advancements in autonomous material handling technologies.

Key words: *brushless motors, encoders, dimensioning*

1. INTRODUCTION

Automated Guided Vehicles (AGVs) are essential in industries requiring efficient and precise material handling and transportation. The performance of an AGV heavily depends on the design and dimensioning of its drive system and navigation components. Proper selection and integration of these systems ensure the vehicle meets operational demands while maintaining reliability and accuracy [1], [7]. This paper focuses on the rationale behind choosing a differential drive system with brushless motor wheels for the AGV. These motors offer a balance of efficiency, durability, and adaptability for autonomous navigation [3], [9]. The dimensioning process considers critical factors such as payload, terrain conditions, and performance requirements like torque and speed [1], [9]. To improve odometry accuracy and address potential wheel slippage, a dead wheel encoder is incorporated into the design. The encoder selection emphasizes resolution and placement to enhance position tracking and control [2], [6]. By detailing the decision-making and design processes, this study provides insights into developing a robust and efficient AGV platform [5], [12]. This design approach reduces both initial and ongoing costs, making AGVs more accessible and practical for a wider range of applications [8], [13].

---

*Corresponding author

2. CHOOSING THE TRACTION SYSTEM AND MOTOR TYPE

For the traction system, it was opted for a differential traction design complemented by four caster wheels to enhance the stability of the platform. Differential traction allows independent control of two drive wheels, enabling precise navigation, tight turns, and smooth operation, which are essential for autonomous applications[1], [4]. The addition of caster wheels provides balance and stability, preventing the platform from tipping and ensuring consistent performance on uneven surfaces. The drive wheels are mounted on a suspension system[9], [11].

For the motor type, it was chosen the gearless brushless hub motor for its high reliability, as it has fewer moving parts, reducing mechanical failure. It requires minimal maintenance due to the lack of gears and brushes. The motor operates quietly, eliminating gear noise, which is ideal for noise-sensitive environments [3], [7]. It provides a fast response to acceleration and deceleration commands, improving maneuverability. The design is highly efficient, with reduced mechanical losses, and compact, saving space and reducing the robot's weight. These features make it the perfect choice for the robot's traction system[2],[6].

3. DIMENSIONING THE TRACTION SYSTEM OF THE ROBOT

To enable the robot's movement, selecting appropriate motors is crucial, as they are a core component of this project. The forces acting on the robot were considered, influencing the required torque and power to ensure platform mobility[4], [5]. Before calculating the motor specifications for the AGV, brushless hub motors commonly used in hoverboards were evaluated. Based on this, the external wheel diameter and wheel mass were chosen, as detailed below[6], [10].

Initial Data:

- Vehicle mass: m1=60 kg
- External wheel diameter: D1=168 mm
- Wheel mass: mD1=3.1 kg/pc
- Number of wheels: n1=2 pc
- Rolling friction coefficient (wheel to floor): μ1=0.013
- System efficiency: η=85%
- Maximum floor slope angle: α=10∘
- Operating speeds: V1=60 m/min,V2=180 m/min
- Acceleration/deceleration time: t1=4 s
- Stopping precision: Δl=2 mm
- Safety factor: Fs=1.5

Mathematical model:

Robot Inertia

The total inertia of the robot is calculated using Equation (1):

$$J_R = (m_1 + (1/2)\, m_{D1} \times n_1) \times (D_1 \times 10^{-3} / 2)^2 \quad (1)$$
$$J_R = (60 + (1/2)\, 3.1 \times 2) \times (168 \times 10^{-3} / 2)^2$$
$$J_R = 0.4452\ \text{kg·m}^2$$

Required Speeds

The rotational speeds corresponding to the operating speeds are calculated as:

$$Vm1 = (V1) / (\pi\, D1 \times 10\text{-}3) \quad (2)$$
$$Vm1 = 60 / (3.14 \times 168 \times 10\text{-}3)$$
$$Vm1 = 113.7\ \text{r/min}$$

$$Vm2 = (V2) / (\pi\, D1 \times 10\text{-}3) \quad (3)$$
$$Vm2 = 180 / (3.14 \times 168 \times 10\text{-}3)$$
$$Vm2 = 314.2\ \text{r/min}$$

Acceleration Torque
The torque required for acceleration is calculated using Equation (4):

$$A = JR\,(\,Vm / (\,9.55 \times t1\,)) \tag{4}$$

$$A = 0.4452 \times (\,341.2 / (\,9.55 \times 4\,))$$
$$A = 3.977\ \text{Nm}$$

Load Torque
The force required to overcome rolling and slope resistance is calculated using:

$$F = 9.8\,(\,(\,m\,1 + n1 \times m\,D1\,) \times (\,\sin\alpha + \mu1 \cos\alpha\,) \times (\,\sin\alpha + \mu2 \cos\alpha\,)\,) \tag{5}$$
$$F = 9.8\,(\,(\,60 + 2 \times 3.1\,) \times (\,\sin 10 + 0.013 \times \cos 10\,) \times (\,\sin 10 \times \cos 10\,)\,)$$
$$F = 121\ \text{N}$$

$$TL = (\,F \times D1 \times 10\text{-}3\,) / (2\,\eta \times 0.01\,) \tag{6}$$
$$TL = (\,121 \times 168 \times 10\text{-}3\,) / (2 \times 85 \times 0.01\,)$$
$$TL = 11.95\ \text{Nm}$$

Total Torque
The total required torque is:

$$T = (\,Ta + TL\,) \times Fs \tag{7}$$
$$T = (\,3.977 + 11.95\,) \times 1.5$$
$$T = 23.90\ \text{Nm}$$

Individual motor torque
Thus, each motor must provide a torque of:

$$Tmotor = T / 2 = 23.9 / 2 = 11.945\text{Nm} \tag{8}$$

Considering the calculated torque requirement, two 6.5-inch hoverboard motors with a nominal power of 350W and a maximum torque of 13.21 Nm were selected. These motors are brushless, mounted in the wheels, and suitable for the design due to their high efficiency, compact form factor, and robust performance.

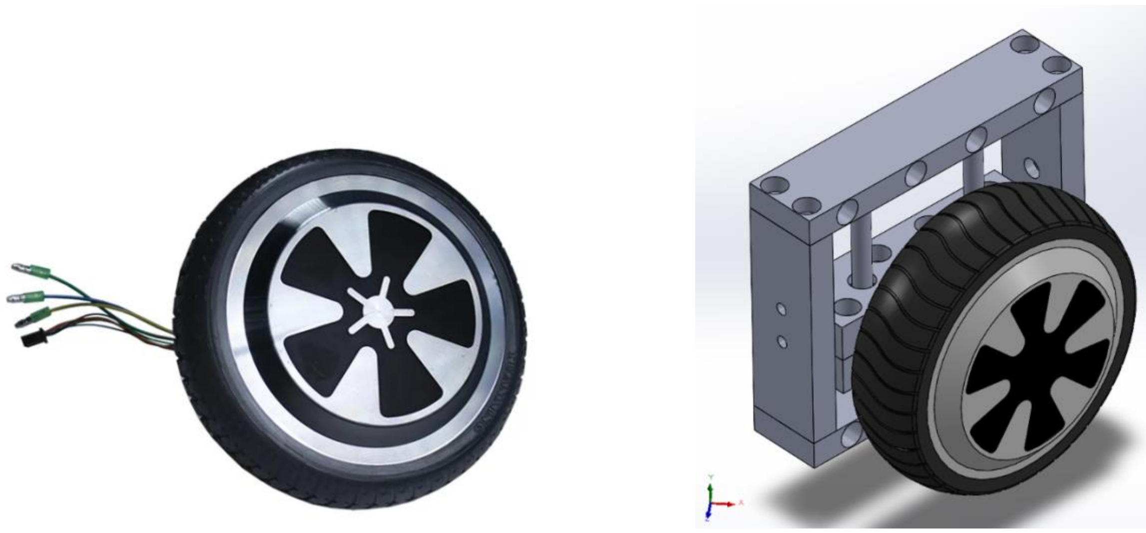

Figure 1: Motor wheel used

Key Specifications of the 6.5" Hub Motor with Encoder
- Operating voltage: 12–36 VDC
- Encoder voltage: 5 VDC
- Nominal power: ~ 350W

- No-load speed: 600 RPM @ 36 VDC
- Loaded speed: 60 RPM @ 36 VDC
- Maximum speed: 15 km/h
- Motor weight: 3.1 kg

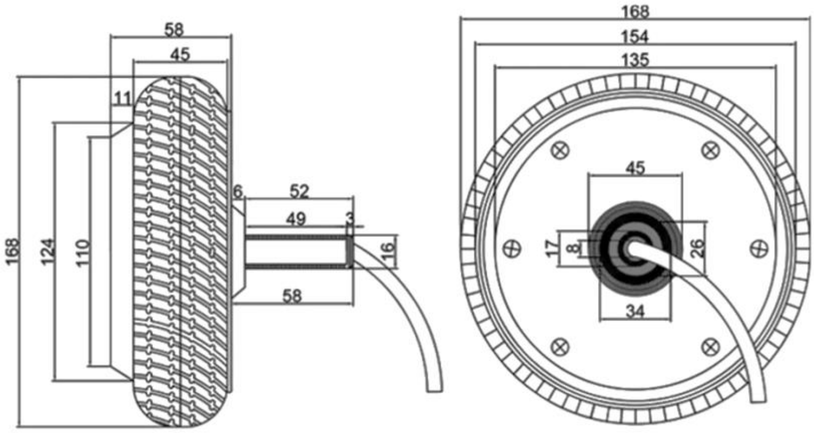

Figure 2: Motor wheel dimension

Table 1: Motor Performance

Typical Performance	V	A	W	Nm	rpm
No Load	36.07	0.987	35.60	0.03	624.4
Maximum Efficiency	36.08	7.601	274.2	3.91	508.2
Maximum Power	36.07	13.17	478.3	7.59	419.8
Maximum Torque	36.07	13.22	477.1	13.21	120.9

4. CHOOSING AND DIMENSIONING THE ADDITIONAL ENCODERS

Although the motor wheels come with built-in encoders providing 90 pulses per revolution, their resolution is insufficient for the desired stopping precision of 2 mm.

To address the resolution limitation the solution chosen is the using of inert wheels encoders. The encoder wheels will be the same diameter as the motor wheels situated near the motor wheels

Below is the calculation of the stopping resolution based on motor built in encoders and a comparison with the required precision of 2 mm or more.

Wheel Diameter:

$$D = 168 \text{ mm}$$

Wheel Circumference:

$$C = \pi \times D = 3.14 \times 168 \text{ mm} = 527.52 \text{ mm} \quad (8)$$

Number of Pulses per Revolution:

$$P = 90 \text{ pulses}$$

Stopping resolution is calculated as:

$$\text{Stopping Resolution} = C / P \quad (9)$$

$$\text{Stopping Resolution} = 527.52 \text{ mm} / 90 = 5.8613 \text{ mm}$$

Calculation of the Required Number of Pulses for a 2 mm Resolution

To achieve a stopping resolution of 2 mm, the required number of pulses per revolution can be calculated as:

$$\text{Required Number of Pulses} = \text{Wheel Circumference} / \text{Desired Resolution} \quad (10)$$
$$\text{Required Number of Pulses} = 527.52\ \text{mm} / 2\ \text{mm} = 263.76\ \text{pulses}$$

Rounding up to the nearest whole number, the encoder must have at least 264 pulses per revolution to achieve a stopping resolution of 2 mm.

To address the resolution limitation, I selected two optical encoders with 500 pulses per revolution, model 38S6G5-500-G24N.

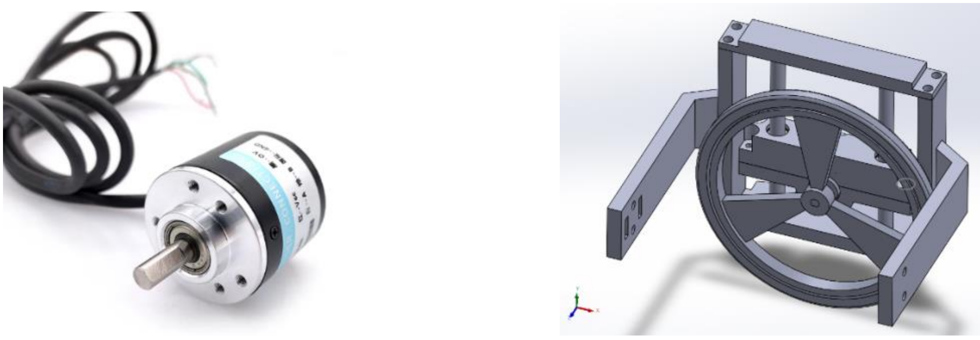

Figure 3: 38S6G5-500-G24N Encoder

Determining the Theoretical Maximum Stopping Resolution with a 500-Pulse Encoder

To calculate the theoretical maximum stopping resolution using an encoder with 500 pulses per revolution, the same wheel dimensions are used:

Wheel Diameter:

$$D = 168\ \text{mm}$$

Wheel Circumference:

$$C = \pi \times D = 3.14 \times 168\ \text{mm} = 527.52\ \text{mm} \quad (11)$$

Number of Pulses per Revolution:

$$P = 500\ \text{pulses}$$

Stopping resolution is calculated as:

$$\text{Stopping Resolution} = C / P \quad (12)$$
$$\text{Stopping Resolution} = 527.52\ \text{mm} / 500 = 1.055\ \text{mm}$$

The theoretical maximum stopping resolution of 1.055 mm using a 500-pulse encoder is significantly smaller than the desired stopping resolution of 2 mm, ensuring sufficient precision for controlling the AGV.

The entire developed mobile robot is presented in the below figure.

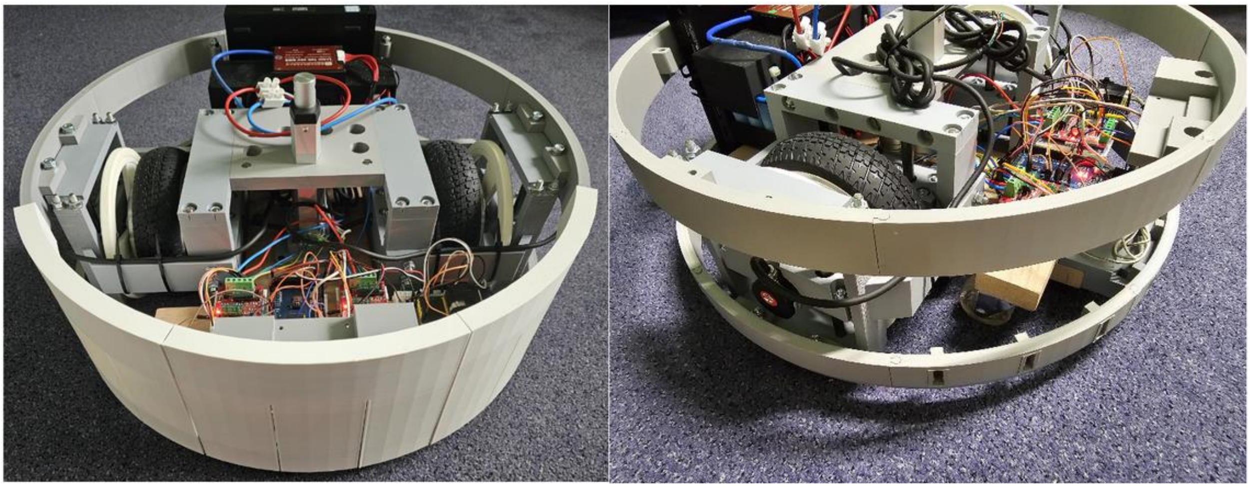

Figure 4: Developed Automated Guided Vehicle

5. CONCLUSIONS

The study presented a thorough approach to the selection and dimensioning of key components for the Automated Guided Vehicle (AGV) traction system, emphasizing the importance of a differential drive system and advanced encoder integration. The differential drive system was chosen due to its simplicity, precision, and ability to adapt to diverse operational environments, making it a practical and versatile solution for industrial applications. The integration of brushless hub motors was pivotal in achieving the desired performance metrics. These motors provided high reliability, required minimal maintenance, and demonstrated compactness and energy efficiency. Their performance capabilities, including meeting specific torque and speed requirements, underscore their suitability for the AGV platform.

A significant enhancement in odometry accuracy was achieved by addressing the limitations of built-in motor encoders. This was accomplished by incorporating additional optical encoders with 500 pulses per revolution mounted on dead wheels. This configuration overcame wheel slippage issues, delivering a stopping resolution of 1.055 mm, which is considerably better than the targeted 2 mm threshold. This precise navigation capability ensures the AGV's reliability in applications demanding high positional accuracy.

Moreover, the design and dimensioning approach emphasized cost-effectiveness, scalability, and robustness. The system's modularity supports easy upgrades and maintenance, aligning with the evolving needs of industrial environments. The detailed calculations and design insights provided in this study serve as a foundation for developing reliable, efficient, and future-ready AGVs.

This work not only advances the technical capabilities of AGV systems but also highlights an effective methodology for designing autonomous mobile robots tailored to specific industrial needs. Future work could explore further optimizations, such as integrating advanced control algorithms and alternative sensor technologies, to enhance the platform's adaptability and intelligence in dynamic environments.

References

1. Imanian, F., and Ahmadian, A. "Design and Control for Differential Drive Mobile Robot," *International Journal of Engineering Research & Technology*, Vol. 6, Issue 10, (2017).
2. B. Zhang and H. P. Gavin, "Computationally Efficient Tracking Control of Differential Drive Wheeled Mobile Robots," *2023 American Control Conference (ACC)*, San Diego, CA, USA, 2023, pp. 891–896.
3. Arkn, R.C. *Behavior-Based Robotics*, MIT Press, 5th edition, Editors eds., City, State, (1998).
4. C. Wang, J. Ji, Z. Miao, and J. Zhou, "Synchronization control for networked mobile robot systems based on udwadia–kalaba approach," *Nonlinear Dyn*, Vol. 105, No. 1, pp. 315–330, (2021).
5. H. Nguyen, J. Morrell, K. Mullens, A. Burmeister, S. Miles, N. Farrington, K. Thomas, and D. Gage, “Segway robotic mobility platform,” *Proc. of SPIE - The International Society for Optical Engineering*, Philadelphia, PA, USA, October 27–28, 2004.

6. J. Elke, J. Pei, R. J. Caverly, and D. G. Egziabher, “A low-cost and low-risk testbed for control design of launch vehicles and landing systems,” *Proc. of IEEE Aerospace Conference*, Big Sky, MT, USA, pp. 1–12, 2021.
7. K. M. Lynch and F. C. Park, *Modern Robotics: Mechanics, Planning, and Control*, The Cambridge University Press, (2017).
8. Sever-Gabriel Racz, Mihai Crenganiş, Radu-Eugen Breaz, Adrian Maroşan, Alexandru Bârsan, Claudia-Emilia Gîrjob, Cristina-Maria Biriş, Melania Tera, "Mobile Robots—AHP-Based Actuation Solution Selection and Comparison between Mecanum Wheel Drive and Differential Drive with Regard to Dynamic Loads," *Machines*, Vol. 10, No. 10, pp. 886, (2022).
9. Khatoon, S., Istiyaque, M., & Wani, S. A. "Design Kinematics and Control for a Differential Drive Mobile Robot." *Renewable Power for Sustainable Growth*, Springer, pp. 189–196, (2021). DOI: 10.1007/978-981-33-4080-0_18.
10. Dogra, A., Mahna, S., Padhee, S. S., & Singla, E. "Unified Modeling of Unconventional Modular and Reconfigurable Manipulation System." *arXiv preprint arXiv:2111.11143*.
11. Ali, A. M., Shen, C., & Hashim, H. A. "A Linear MPC with Control Barrier Functions for Differential Drive Robots." *arXiv preprint arXiv:2404.10018*.
12. Karunakaran, H., & Subbaraj, G. R. "Trajectory Control for Differential Drive Mobile Manipulators." *arXiv preprint arXiv:2304.00122*.
13. robolaunch. "Cloudy Mini-AGV: A New ROS 2 Based Open-Source Educational Robot." https://discourse.ros.org/t/a-new-ros-2-based-open-source-educational-robot/31341.